International Journal of Heat and Technology
Vol. 40, No. 5, October, 2022, pp. 1175-1185
Journal homepage: http://iieta.org/journals/ijht

Heat Transfer and Mixed Convection Flow of Non-Newtonian Thermo-Dependent Power Law Fluids with Thermal Radiation Effect

Ilham Erritali[1], Mourad Kaddiri[1], Ismail Arroub[2*], Hamza Daghab[1]

[1] Industrial Engineering Laboratory (LGI), Faculty of Sciences and Technologies, Sultan Moulay Slimane University, B.P. 523, Béni-Mellal 23000, Morocco
[2] Research Laboratory in Physics and Sciences for Engineers (LRPSI), Polydisciplinary Faculty, Sultan Moulay Slimane University, B.P. 592, Béni-Mellal 23000, Morocco

Corresponding Author Email: ismail.arroub@gmail.com

https://doi.org/10.18280/ijht.400508

Received: 19 July 2022
Accepted: 13 October 2022

Keywords:
numerical study, mixed convection, non-Newtonian power law fluids, thermo-dependent viscosity, thermal radiation, lid-driven square cavity

ABSTRACT

The current study explores numerically mixed convection of thermo-dependent power-law fluids in a square lid-driven enclosure, including the thermal radiation effect. The vertical sidewalls are sustained at both hot and cold temperatures. On the other hand, the cavity is insulated from the horizontal walls. The upper wall is moving along the x-axis. The main governing equations that the Boussinesq approximation is used for are solved using the finite difference method. The simulations focus on the effects of multiple pertinent parameters, including the Richardson number. (Ri = 0.1, 1, 10 and 100), thermal radiation parameter (R_d = 0 and 10), power-law index ($0.6 \leq n \leq 1.4$) and the Pearson number ($0 \leq m \leq 6$). The findings reveal that improving the Richardson number reduces heat transfer. Then, increasing R_d results in a domination of heat conduction for a fluid having a higher thermal conductivity. Also, the growth in the power law-index reduces heat transfer while improving convective flow. Finally, increasing the Pearson number improves the convective flow rate and also the average Nusselt number.

1. INTRODUCTION

For many years, the study of both free and forced convection heat transfer inside driven-cavities has been an important engineering problem owing to its industry applications including electronic devices cooling, food processing, crystal growth, glass fabrication [1], lake dynamics [2], solar energy systems, thermal insulation, nuclear reactors [3], lubricating technologies, and many others. Mixed convective flow happens in closed cavities because of a combination of shear force produced by wall movement and buoyancy caused by heat gradient. This phenomenon is governed by non-dimensional parameters like the Grashof number, Gr, and the Reynolds number, Re, which describe buoyancy and shear effects, respectively. Several heat transfer and mixed convective flow investigations have been previously undertaken, using various temperature gradient and enclosure geometries combinations [4-10]. Torrance et al. [11] examined numerically fluid motion caused by a shifting upper wall inside a rectangular enclosure. They revealed that the enclosure's secondary circulation enhances when the aspect ratio increases. Iwatsu et al. [12] analyzed numerically heat transfer and mixed convective flow within a square driven-cavity that was differentially heated from horizontal walls and insulated from vertical walls. Heat transfer is reported to be intensive for large Richardson numbers. Khanafer and Chamkha [13] used numerical simulations to investigate mixed convection inside a driven-cavity filled with a fluid-saturated porous medium. They concluded that the Darcy and Richardson numbers are significant characteristics in convective flows. Aydm [14] simulated laminar mixed convection inside a square cavity that was differentially heated with the left wall moving to the top. As the value of Gr / Re^2 increased, three distinct heat transfer regimes were defined: forced, mixed and free convection. The opposing-buoyancy case's mixed convection range was observed to be significantly higher than the aiding-buoyancy case's. Ouertatani et al. [15] explored numerically 3D mixed convection flow and heat transfer inside a double lid-driven cubic cavity heated from the upper wall and cooled from the bottom wall. They found that with two moving lids, the estimated average Nusselt number was larger than with one moving lid. Sivakumar et al. [16] conducted numerical simulations to investigate the impact of heating location and size on heat transfer and mixed convection fluid flow in driven-cavities. The findings reveal that the heating location has a substantial influence on the flow field. Furthermore, a better heat transfer rate is obtained by minimizing the heating portion in the hot wall. In a lid-driven enclosure with a modified heated wall, Yapici et al. [17] examined laminar mixed convective heat transfer. They observed that with lower Ri, the average Nusselt number gradually enhances with raising amplitude. Nosonov and Sheremet [18] analyzed numerically conjugate heat transfer and mixed convective flow inside an open cavity with different-sized local heaters. They proved that increasing the Richardson number promotes convection inside the enclosure to intensify as the form of the forced flow changes. Gangawane and Oztop [19] conducted a numerical investigation to explore the thermal and flow characteristics of a non-Newtonian fluid generated by mixed convection in a semi-oval driven-cavity. They concluded that raising the Richardson number decreases the heat transfer rate

and at low Richardson numbers, the power-law index has a considerable impact on hydrodynamic properties.

On the other hand, notwithstanding the fact that the majority of fluids utilized in both industrial and domestic applications exhibit non-Newtonian behavior, very few studies have been undertaken to explore the effects of non-Newtonian fluids. owing to its applicability in diverse fields, the non-Newtonian fluids convective flow has been investigated throughout latest years [20-26]. For various power-law indexes n, Akçay et al. [27] examined numerically the boundary layer problem of non-Newtonian fluid flow with fluid injection on a semi-infinite flat plate, with a moving wall in the opposite direction of the uniform mainstream. They reported that the wall mass injection can diminish the viscous drag of the flat plate for all power-law index values excluding (n = 0.01), where the drag reduction degree was minimal. Khani et al. [28] investigated an analytical solution for cooling turbine disks with a non-Newtonian viscoelastic fluid using the homotopy analysis method (HAM). It was shown that viscoelastic fluids exhibit significant rates of heat transfer while minimizing drag. Furthermore, non-Newtonian fluids are widely found in several other fields, including food processing and medical science (blood flow). The problem of non-Newtonian fluid-food particle heat transfer inside the holding tube involved in aseptic processes was conducted numerically by Krishnan and Aravamudan [29]. They revealed that the pseudo-plastic fluids power-law index had a substantial impact on both heat transfer and hydrodynamics at the fluid particle interface. Foong et al. [30] analyzed the blood flow inside the artery numerically. The findings indicate that the rate of heat transfer in blood flow with Newtonian behavior is greater than that with non-Newtonian behavior. In addition, Newtonian blood flow had a lower temperature than non-Newtonian blood flow.

Moreover, Thermal radiation is important in considering several engineering systems. Some researchers [31, 32] have performed many heat transfer research inside a cavity with thermal radiation. Badruddin et al. [33] examined the impacts of viscous dissipation and thermal radiation on heat transfer inside a porous cavity. They observed that by increasing the thermal radiation parameter, both the local and average Nusselt numbers improved at the cavity's hot and cold walls. In the presence of mass transfer, Prasad et al. [34] investigated numerically the radiation effects along an impulsively initiated vertical plate. They reported that as the time t rises, the fluid's velocity and temperature near the plate increases significantly, which is completely missing in the absence of radiation effects. In addition, the average Nusselt number improves as the radiation parameter is enhanced. In a wavy box, Mansour et al. [35] explored the effect of thermal radiation on natural convection. They concluded that enhancing the radiation parameter values raised the averaged Nusselt number. Sheremet [36] demonstrated in their numerical study of viscoelastic fluid free convection with a radiation effect in a square enclosure that raising the radiation parameter rises the rate of heat transfer and intensifies the convective flow rate. In addition, at large values of the thermal radiation parameter, heat conduction is the dominant heat transfer mode.

Otherwise, the real fluid inside cavities has a varied viscosity in many practical applications. As a result, in order to control and intensify technological processes, the influence of varying viscosity on heat transfer and fluid flow must be investigated. Furthermore, the large majority of previous studies has focused on Newtonian fluids [37-43]. Bottaro et al. [44] explored the onset of two-dimensional convection with viscosity that is strongly temperature dependent for an Arrhenius-law fluid. It was demonstrated that when the Rayleigh number Ra exceeds R_C, supercritical steady rolls develop firstly, and that at reasonably large Ra values, a secondary Hopf bifurcation associated to pulsating cells appears. Astanina et al. [45] explore numerically transitory natural convection inside a non-Darcy porous enclosure with temperature-dependent viscosity. They discovered that enhancing the variable viscosity parameter results in the rise of heat transfer and convective flow, as well as the creation of a single-core convection cell for the porous cavity. Alim et al. [46] analysed the impacts of thermo-dependent viscosity and a volumetric heating element on free convection flow across a wavy surface simultaneously. It was reported that as the viscosity variation parameter is raised, the frictional force on the wall increases, whereas the rate of heat transfer decreases greatly. Umavathi and Ojjela [47] explored the influence of varying viscosity on free convection within a vertical rectangular duct filled with a Newtonian fluid. They demonstrated that negative values of the variable viscosity parameter represent the intensive velocity pattern in the duct's left half, whereas positive values of the variable viscosity parameter characterizes the intensive velocity pattern in the duct's right half. However, to the best of our knowledge, just few investigations have been carried with non-Newtonian fluids. Amoura et al. [48] in their numerical study relating to thermal convection of thermo-dependent fluid located between two coaxial cylinders showed that the thermo-dependence of the fluid has no influence on the thermal field for Reynolds numbers between 150 and 300. Solomatov and Barr [49] explored how the initial perturbation form influences the convection onset in non-Newtonian fluids with substantially thermo-dependent power-law viscosity. They revealed that the most efficient thermal perturbations in promoting convective flow (optimal perturbations) are detected in the rheological sublayer at the weakest viscosity region of the fluid layer. Kaddiri et al. [50] simulated numerically steady Rayleigh-Bénard convection of non-Newtonian thermo-dependent power-law fluids inside a square enclosure. Thermo-dependence was shown to improve flow in the rheological sublayer while decreasing heat transfer.

However, the bibliography review reveals a dearth of works that investigate at the same time the impact of thermo-dependence and thermal radiation on heat transfer and fluid flow inside driven-enclosures. To fill that need, and considering the relevance through using non-Newtonian fluids and driven lids in confined cavities enclosures as heat transfer improvement techniques for exceeding performance efficiency limits in a variety of industrial applications. The purpose of this study is to explore numerically mixed convection flow of non-Newtonian thermo-dependent power-law fluids in a square lid-driven cavity with thermal radiation effect. The influences of important parameters on heat transfer and fluid flow characteristics, like the Richardson number, thermal radiation, power law index, and Pearson number, are explored and explained.

2. PROBLEM DESCRIPTION

The physical configuration and corresponding boundary conditions under consideration in the ongoing study are depicted in Figure 1. It consists of a square lid-driven cavity

of dimension L' × L', the upper wall moves back to the right at a steady velocity of u'_0. The left and right walls are sustained at hot and cold temperatures T'_H and T'_C, respectively, where ($T'_H > T'_C$). While the horizontal walls are insulated.

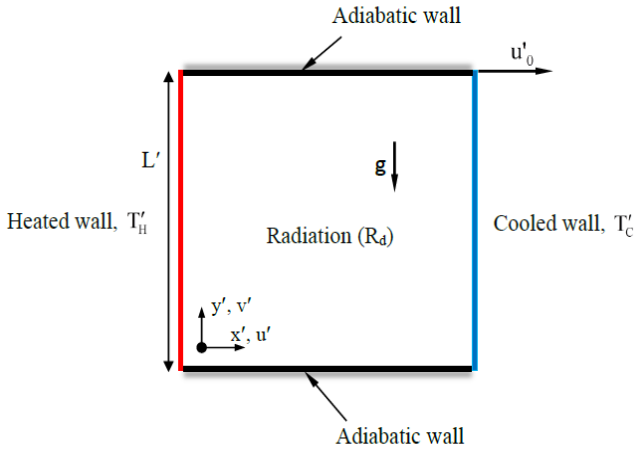

Figure 1. Geometry of the cavity and boundary conditions

The cavity contains non-Newtonian power law fluids with thermo-dependent rheological behavior that can be approximated using the Ostwald-De Waele model. As regards the apparent laminar viscosity, it can be stated as:

$$\mu'_a = K_T\left[2\left[\left(\frac{\partial u'}{\partial x'}\right)^2+\left(\frac{\partial v'}{\partial y'}\right)^2\right]+\left(\frac{\partial u'}{\partial x'}+\frac{\partial v'}{\partial y'}\right)^2\right]^{(n_T-1)/2} \quad (1)$$

where, the empirical factors n_T and k_T denote respectively the indices of power-law behavior and consistency. They are, in general, temperature dependent, although in most cases the temperature dependency of n_T can be neglected (n_T = n) because it is weak in comparison to that of K_T [51, 52]. This can be stated using the exponential law [53]:

$$K_T = k\exp\left(-b\left(T'-T'_r\right)\right) \quad (2)$$

Thermo-dependency parameter and the consistency index at T'_r the reference temperature are denoted by *b* and *k*, respectively. Furthermore, for n < 1, the apparent viscosity reduces as the shear rate rises, showing shear-thinning (or pseudo-plastic) behavior. In contrast, when n > 1, the fluid is termed as shear-thickening (or dilatant) because the apparent viscosity enhances as the shear rate rises. For n = 1, the behavior is Newtonian $K_T = \mu_a$ (constant viscosity).

Despite the fact that the power-law model accurately describes the rheological behavior of numerous materials over a wide shear rates range (or shear stresses), it has the advantage of being simple, which supports its usage in vast theoretical studies of fluids with shear-thinning or shear-thickening behaviors.

For this investigation, we used the following simplifying assumptions:

- The flow is known as laminar because the fluid motion is slower owing to the minor gradients imposed on the enclosure [54].
- The fluid is supposed to be incompressible. At pressures near to atmospheric pressure, liquids are an excellent approximation to incompressible fluids.
- The effects of viscous dissipation are negligible.
- Except for density and viscosity in the buoyancy term, the physical properties of the fluid are thought to be temperature independent. The density is approximated using the Boussinesq approximation [55].
- The fluid flow is thought to be bidimensional, but the third dimension is substantial enough to satisfy this assumption, allowing for a better comprehension of more complex three-dimensional flows [54].

3. GOVERNING EQUATIONS

Taking into consideration the aforesaid assumptions and employing the typical scales $x = \frac{x'}{L'}$, $y = \frac{y'}{L'}$, $p = \frac{p'}{\rho\, u_0'^2}$, $t = \frac{t'}{L'}u'_0$, $u = \frac{u'}{u'_0}$, $v = \frac{v'}{u'_0}$ and $T = \frac{T'-T'_C}{T'_H-T'_C}$, which stand for length, pressure, time, velocity, and temperature. As a result, the non-dimensional governing 2D equations that characterize system behavior can be stated as follows in terms of the vorticity-stream function Ω-ψ formulation:

$$\frac{\partial\Omega}{\partial t}+\frac{\partial(u\Omega)}{\partial x}+v\frac{\partial(u\Omega)}{\partial y}=\frac{1}{Re}\left[\begin{array}{l}\mu_a\left[\frac{\partial^2\Omega}{\partial^2 x}+\frac{\partial^2\Omega}{\partial^2 y}\right]+\\ 2\left[\frac{\partial\mu_a}{\partial x}\frac{\partial\Omega}{\partial x}+\frac{\partial\mu_a}{\partial y}\frac{\partial\Omega}{\partial y}\right]\end{array}\right]+S_\Omega \quad (3)$$

$$\frac{\partial T}{\partial t}+\frac{\partial(uT)}{\partial x}+\frac{\partial(vT)}{\partial y}=\frac{1}{Re\,Pr}\left(1+\frac{4}{3}R_d\right)\left(\frac{\partial^2 T}{\partial^2 x}+\frac{\partial^2 T}{\partial^2 y}\right) \quad (4)$$

$$\frac{\partial^2\Psi}{\partial x^2}+\frac{\partial^2\Psi}{\partial y^2}=-\Omega \quad (5)$$

As seen below, the dimensionless stream function and vorticity are linked to the non-dimensional velocity components:

$$u=\frac{\partial\Psi}{\partial y}\quad;\quad v=-\frac{\partial\Psi}{\partial x}\quad\text{and}\quad \Omega=\frac{\partial v}{\partial x}-\frac{\partial u}{\partial y} \quad (6)$$

where,

$$\mu_a = e^{-mT}\left[2\left[\left(\frac{\partial u}{\partial x}\right)^2+\left(\frac{\partial v}{\partial y}\right)^2\right]+\left(\frac{\partial u}{\partial x}+\frac{\partial v}{\partial y}\right)^2\right]^{(n-1)/2} \quad (7)$$

$$S_\Omega=\frac{1}{Re}\left[\begin{array}{l}\left(\frac{\partial^2\mu_a}{\partial^2 x}-\frac{\partial^2\mu_a}{\partial^2 y}\right)\left(\frac{\partial u}{\partial y}+\frac{\partial v}{\partial x}\right)-\\ 2\frac{\partial^2\mu_a}{\partial x\partial y}\left(\frac{\partial u}{\partial x}-\frac{\partial v}{\partial y}\right)\end{array}\right]+Ri\frac{\partial T}{\partial x} \quad (8)$$

The corresponding boundary conditions are:

$$u = 1,\ v = 0,\ \frac{\partial T}{\partial y} = 0 \qquad \text{(The upper wall)}$$

$$u = v = 0,\ \frac{\partial T}{\partial y} = 0 \qquad \text{(The lower wall)}$$

$$u = v = 0,\ T = T_H \qquad \text{(The left heated wall)}$$

$$u = v = 0,\ T = T_C \qquad \text{(The right wall)}$$

The preceding equations identified five dimensionless parameters, including Prandtl number Pr, Richardson number Ri, Reynolds number Re, Pearson number m and radiation parameter R_d, which are stated as follows:

$$Pr = \frac{C_p k}{\lambda}\left(\frac{u'_0}{L'}\right)^{n-1};\ Ri = \frac{Gr}{Re^2} = \frac{g\beta(T'_H - T'_C)L'}{u'^2_0};\ Re = \frac{\rho L'^n u'^{2-n}_0}{k}$$

$$m = -\frac{1}{K_T}\frac{dK_T}{dT} = -\frac{d(\ln(K_T/k))}{dT};\ R_d = \frac{4\sigma T_c^3}{\lambda \beta_r} \qquad (9)$$

Using the Rosseland approximation [56, 57] for thermal radiation, we get the radiative heat flux:

$$q_{rx'} = -\frac{4\sigma}{3\beta_r}\frac{\partial T'^4}{\partial x'} \quad ; \quad q_{ry'} = -\frac{4\sigma}{3\beta_r}\frac{\partial T'^4}{\partial y'} \qquad (10)$$

Because it is assumed that differences in temperature within the cavity are too minimal, we can develop T'^4 in Taylor series about T'_C and approximating it, we have:

$$T'^4 \approx 4T' T'^3_C - 3T'^4_C \qquad (11)$$

As a result, the heat flux in the x and y directions owing to radiation is reduced to:

$$q_{rx'} = -\frac{16\sigma T_C^3}{3\beta_r}\frac{\partial T'}{\partial x'} \quad ; \quad q_{ry'} = -\frac{16\sigma T_C^3}{3\beta_r}\frac{\partial T'}{\partial y'} \qquad (12)$$

4. HEAT TRANSFER

The physical quantities of importance in quantifying the heat transfer rate are the local Nusselt number Nu along the heated wall and the average Nusselt number $\overline{Nu}$, which are denoted as:

$$Nu = -\left(1 + \frac{4}{3}R_d\right)\left.\frac{\partial T}{\partial x}\right|_{x=0} \quad ; \quad \overline{Nu} = \int_0^1 Nu\, dy \qquad (13)$$

5. NUMERICAL SOLUTION

The two-dimensional governing equations are numerically solved, using a finite difference approach with a uniform grid size, taking into account the corresponding boundary conditions. The alternating-direction implicit method (ADI) is used to integrate the vorticity and energy equations, Eqs. (3) - (4). This classical method, well adapted to study transient convection problems. Generally, it gives rise to tridiagonal matrices in both directions and the calculation scheme is efficient because it is simple and consistent. Ozoe and Churchill [58] were the first to successfully apply this method, which is commonly used for Newtonian fluids, to non-Newtonian power-law fluids and also was used in several recent studies [59-62]. To satisfy mass conservation, the Poisson equation, Eq. (5), is solved using a point successive over-relaxation method (PSOR) and an optimized relaxation factor obtained using the Franckel model [63].

The convergence criterion $\sum_{i,j}|\Psi^{k+1}_{i,j} - \Psi^k_{i,j}| / \sum_{i,j}|\Psi^{k+1}_{i,j}| < 10^{-5}$ is adopted, where $\Psi^k_{i,j}$ is the value of the stream function at the node (i, j) for the kth iteration level. A regular grid size of (61 × 61) is appropriate for getting satisfactory results. The time step size was changed from 10^{-6} to 10^{-4} depending on the values of the controlling parameters.

6. CODE VALIDATION AND GRID INDEPENDENCE

To check the accuracy of the developed numerical code, our results, reported in terms of the average Nusselt number, are compared with prior research into mixed convection in a cavity. As a result, as indicated in Table 1, a good agreement is generally obtained.

The grid size was chosen to provide the optimal trade-off between computing time and results precision. Table 2 shows the sensitivity of the results to the grid in terms of |Ψmax| and $\overline{Nu}$, as determined by the selected grid (61 × 61) and a finer one (81 × 81). The maximum relative error for |Ψmax| and $\overline{Nu}$ is less than 1.51% and 0.81%, respectively, based on the results shown in this table. In terms of CPU time, the computational effort was also examined for both grids.

For the tested cases, a grid refinement from (61 × 61) to (81 × 81) results in a CPU time increase of more than two times. Hence, the mesh dimension of (61 × 61) is jugged sufficient to conduct the current investigation accurately.

Table 1. Comparison of the average Nusselt number between present results and previous data in the literature for a lid-driven enclosure with Gr = 100 and Pr = 0.71

Re	Ri	Present work	Waheed [4]	Tiwari and Das [7]	Abdelkhalek [9]	Iwastu et al. [12]]	Khanafer and Chamkha [13]	Kefayati [64]
1	100	-	1.00033	-	-	-	-	1.0094
100	0.01	2.05	2.03116	2.10	1.985	1.94	2.01	2.09
400	0.000625	4.38	4.0246	3.85	3.8785	3.84	3.91	4.08082
1000	0.0001	6.68	6.48423	6.33	6.345	6.33	6.33	6.54687

Table 2. Preliminary grid independence tests for m = 3, R_d = 10, Pr = 7 and Gr = 10^4

Grid		61 × 61		81 × 81		101 × 101	
n	**Ri**	$\|\Psi_{max}\|$	$\overline{Nu}$	$\|\Psi_{max}\|$	$\overline{Nu}$	$\|\Psi_{max}\|$	$\overline{Nu}$
0.6	0.1	0.051	47.585	0.051	47.680	0.051	46.047
	10	0.531	54.409	0.535	54.666	0.523	53.860
1	0.1	0.066	49.702	0.067	50.108	0.068	50.350
	10	0.417	38.280	0.417	38.108	0.417	38.180
1.4	0.1	0.094	52.126	0.093	51.966	0.093	51.870
	10	0.342	31.808	0.342	31.688	0.342	31.678

7. RESULTS AND DISCUSSION

Several studies have proved that the Prandtl number, Pr, has a strong influence on mixed convection, as indicated in Refs [65, 66]. However, Lamsaadi et al. [67] and Alloui et al. [68] reveal that natural convection is unaffected by high values of Pr. In the current investigation, the Prandtl / Grashof numbers were kept constant at 7 / 10^4 to minimize the number of controlling parameters.

Therefore, the mixed convection heat transfer flow generated inside the enclosure is governed by the Richardson number Ri which simulates mixed and forced convection dominating regimes, the Pearson number m, the thermal radiation parameter R_d, and the power-law index n.

7.1 Analysis of streamlines and isotherms

Streamlines and isotherms diagrams exhibiting the thermal radiation effect on the dynamical and thermal fields are displayed in Figures 2 - 4. For m = 0, with multiple Ri values and power law index n. Despite of the radiation parameter value, it should be noted that the flow remains, in general, unicellular and clockwise.

As can be observed, raising R_d causes the convective flow to intensify while diminishing the size of the convective cell core. This one appears to be moving from the top cold corner to the center of the cavity. Such changes are promoted by the less intensive heating of the cavity's top side. Moreover, a rise in the thermal radiation parameter results in a weakening of the mechanism of convective heat transfer and an enhancement of heat conduction. In addition, the isotherm distribution indicates both a straightening of the isotherms in the cavity's center and a diminution in the thermal boundary-layers near to the vertical isothermal walls. Furthermore, the impact of Richardson number (mixed convection parameter) on temperature fields and flow is shown to be modest for Ri = 0.1 (dominate forced convection). Whereas, Ri ≥ 1 reveals buoyancy effects owing to the variable density of fluid in the enclosure, which improves convective flow. For various Ri values, the size and position of the convective cell core depend on the power law index n. For n = 0.6 (shear-thinning fluids), the convective cell core appears to be moving toward the moving lid due to the shear force applied by the moving wall. The shear force effect decreases as the power law index rises from 0.6 to 1.4. Therefore, the convective cell core seems to shift from the bottom cold corner to the middle of the moving lid.

The isotherms exhibit a diminution of convection inside the cavity when the isotherm gradient decreases on the hot wall, when Ri increases from 0.1 to 10. Hence, it proves that as the Richardson number rises, heat transfer diminishes. Moreover, the isotherms become more tightened on the hot wall when n increase from 0.6 to 1.4, which leads to an increase in the hot wall's gradient temperature. Also, this reflects the improvement of heat transfer as the power-law index increases. Kefayati [64] makes the same observations.

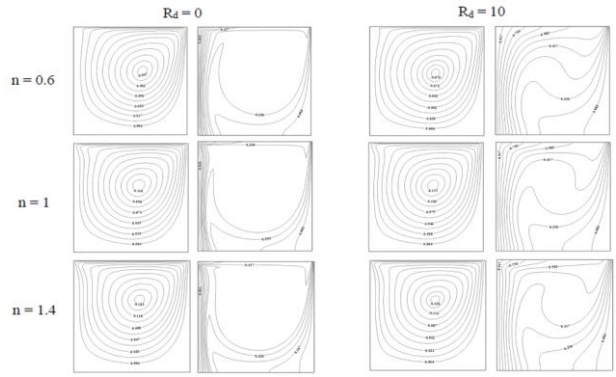

Figure 2. Streamlines (left) and isotherms (right), for m = 0 and Ri = 0.1 with different values of n and R_d

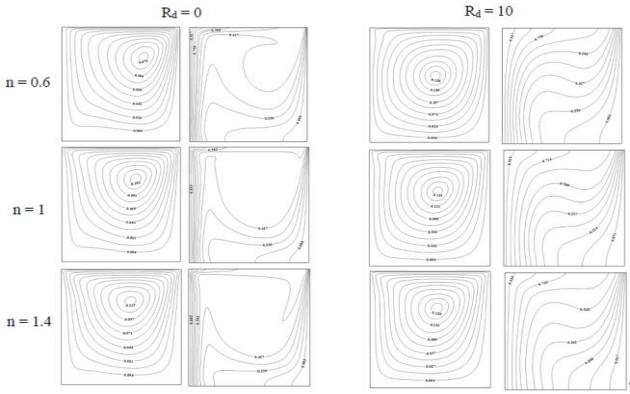

Figure 3. Streamlines (left) and isotherms (right), for m = 0 and Ri = 1 with different values of n and R_d

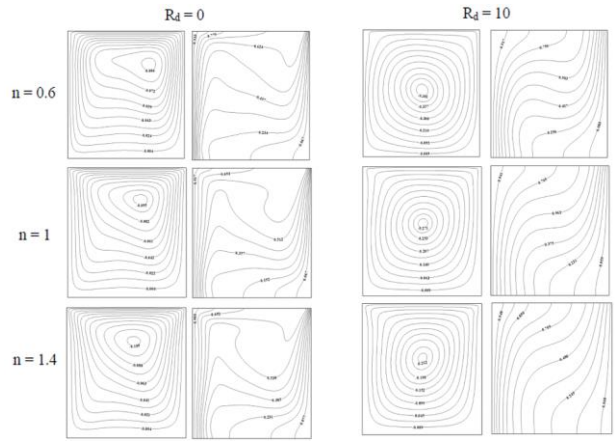

Figure 4. Streamlines (left) and isotherms (right), for m = 0 and Ri = 10 with different values of n and R_d

In order to investigate the impact of temperature-dependent viscosity on dynamical and thermal fields, representative streamlines and temperature contours are shown in Figures 5 - 7. For n = 0.6, Ri = 0.1, Ri = 10 and several values of m and R_d. The influence of m can be evaluated using the values of m, R_d, and Ri.

For Ri = 0.1 (dominate forced convection), as indicated, the flow is clockwise and unicellular. With a growth of m the flow becomes double-cellular and clockwise.

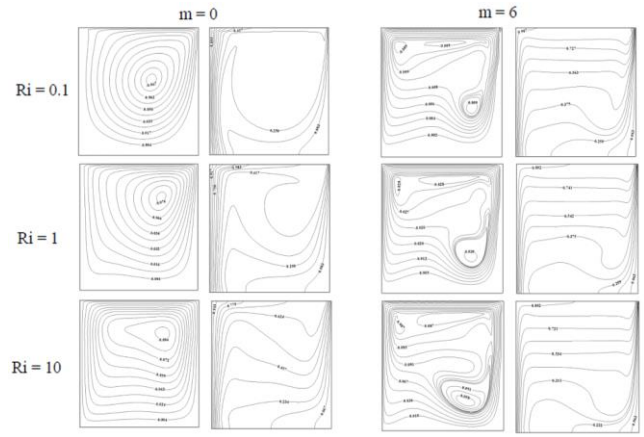

Figure 5. Streamlines (left) and isotherms (right), for n = 0.6 and R_d = 0 with different values of m and Ri

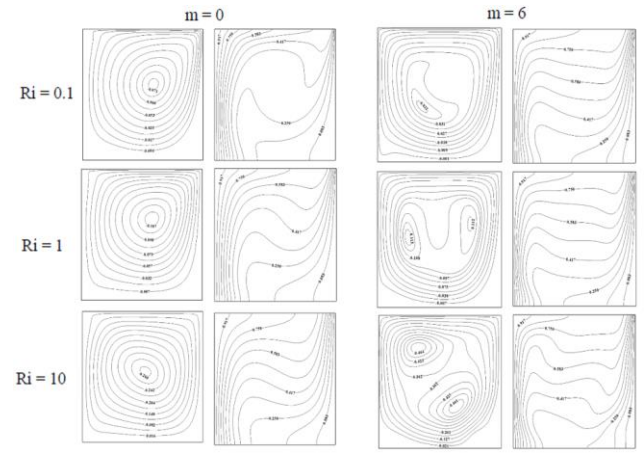

Figure 6. Streamlines (left) and isotherms (right), for n = 0.6 and R_d = 5 with different values of m and Ri

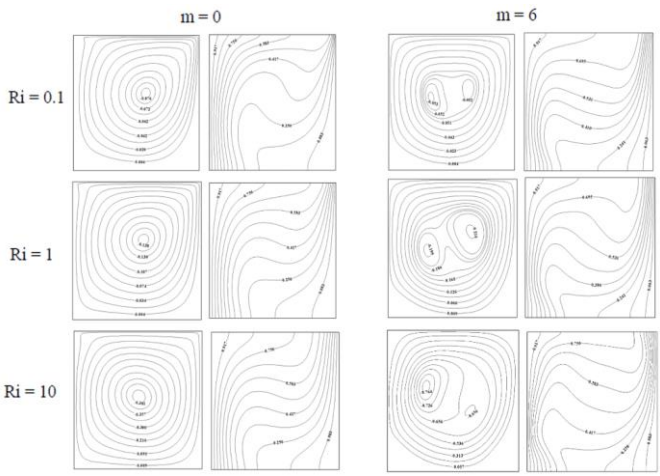

Figure 7. Streamlines (left) and isotherms (right), for n = 0.6 and R_d = 10 with different values of m and Ri

Moreover, it appears clear that the convective cell core is moved to the side of the hot wall. Also, the streamlines become tighter and tighter as they approach the heated wall, at which the effective viscosity is low. This leads to severe convection in this area while also causing a stagnation zone in the high viscosity regions. As for the isotherms, the high temperature from the left hot wall penetrates the enclosure more intensely along the top isothermal wall, whereas the low temperature penetration from the right cold wall reduces. These changes are due to more intense movement of the low viscosity fluid in the high temperature regions.

For Ri = 10 (dominant natural convection), the flow structure has the same aspect of Ri = 0.1. Moreover, the streamlines tend to be tighter near the hot wall when m is increased to 6. An examination of the isotherms shows that their deviations become more and more significant near the two walls (cold and hot). This distortion is due to the competition between the two flow modes due to the gain or evacuation of the heat transfer near these walls. Also, leads to the conclusion that natural convection dominates forced convection.

7.2 Analysis of heat transfer rate and flow intensity

The evolutions of fluid flow characteristics $\overline{Nu}$ and $|\Psi max|$ with the Richardson number Ri, are depicted in Figure 8, for m = 0 and various R_d and n.

As displayed in this figure, for R_d = 0 there is a critical point where the power law index's effect is reversed. This is clear that for lower values of Ri (dominate forced convection) the average Nusselt number $\overline{Nu}$ and flow intensity $|\Psi max|$ are both enhanced by increasing the power law index. However, it exhibits that for high values of Ri (dominant free convection) the flow intensity $|\Psi max|$ and the average Nusselt number produce an opposite effect.

On the other hand, regardless of the power law index value, enhancing the Richardson number decreases the average Nusselt number and improves flow intensity. This behavior results from the predominance of natural convection accompanying the intensification of the cellular flow manifested by the increase in $|\Psi max|$. Moreover, the forced convection is low therefore the speed of the lid is low which reduces the heat transfer at the active walls. Because buoyancy forces are stronger than viscous forces. Furthermore, the increase in R_d increases heat transfer and the fluid flow in the cavity. Also, the critical point is moved to lower Richardson number values.

The variations of $\overline{Nu}$ and $|\Psi max|$ with thermal radiation R_d are presented in Figure 9, for n = 0.6, with various Ri and m values. First, it is easy to observe that. $\overline{Nu}$ and $|\Psi max|$ are increasing functions of R_d, because of the buoyancy effects that promote convection.

For Ri = 0.1, an improvement in the Pearson number m increases the convection process, which is reflected in the rise of the average Nusselt due to the weakening of apparent viscosity. While, the augmentation of m decreases the flow intensity $|\Psi max|$, which means that the flow circulation inside the cavity weakens for small Ri values because of the viscous forces.

For Ri = 10, the growth of the Pearson number m augments $\overline{Nu}$ and ameliorate the convective flow within the cavity, as indicated by the rise of the maximum absolute value of stream function $|\Psi max|$.

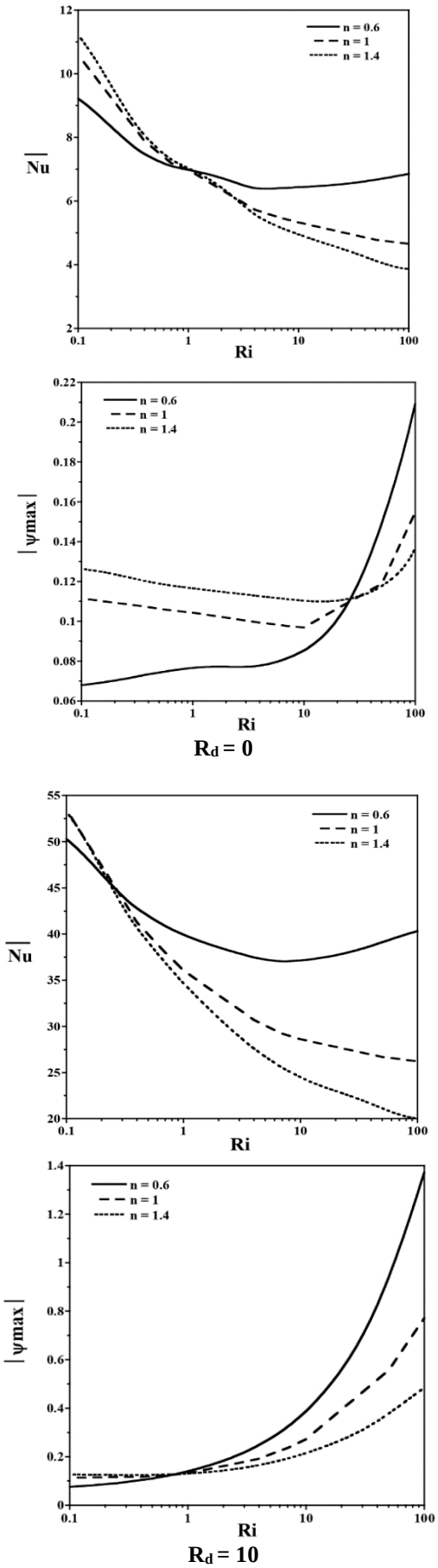

Figure 8. Variations, with Ri, of the average Nusselt number, $\overline{Nu}$, and the maximum value of the stream function, |Ψmax|, for m = 0 and various values of R_d and n

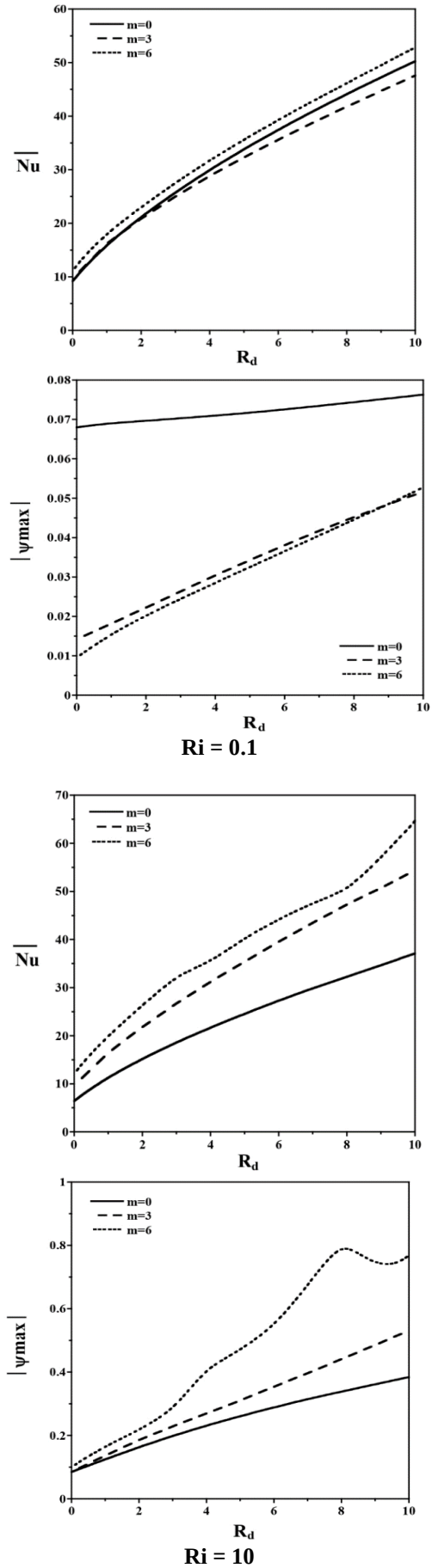

Figure 9. Variations, with R_d, of the average Nusselt number, $\overline{Nu}$, and the maximum value of the stream function, |Ψmax|, for n = 0.6 and various values of Ri and m

8. CONCLUSIONS

A numerical investigation is conducted in this study to explore the combined effect of thermal radiation and thermo-dependent viscosity on non-Newtonian power law fluids mixed convection in a square driven-cavity, based on the results, we reach the following conclusions.

- Because of buoyancy forces being greater compared to viscous forces, heat transfer reduces as the Richardson number enhances for various power law indexes.
- As the power law index increases, heat transfer diminishes but convective flow improves.
- Increasing the thermal radiation parameter R_d causes the convective flow to enhance as well as the convective cell core size to diminish. Heat conduction also dominates the heat transfer process for high R_d values.
- The improvement of the Pearson number m leads to the movement of the convective core close the side of the hot wall. Moreover, the convective flow rate and the average Nusselt number increase with the rise of the viscosity variation parameter.

REFERENCES

[1] Pilkington, L.AB. (1969). Review lecture. The float glass process. Proceedings of the Royal Society A: Mathematical, Physical and Engineering Sciences, 314(1516): 1-25. http://dx.doi.org/10.1098/rspa.1969.0212

[2] Imberger, J., Hamblin, P.F. (1982). Dynamics of lake reservoirs and cooling ponds. Annual Review of Fluid Mechanics, 14(1): 153-187. http://dx.doi.org/10.1146/annurev.fl.14.010182.001101

[3] Ideriah, F.J.K. (1980). Prediction of turbulent cavity flow driven by buoyancy and shear. Journal of Mechanical Engineering Science, 22(6): 287-295. http://dx.doi.org/10.1243/jmes_jour_1980_022_054_02

[4] Waheed, M.A. (2009). Mixed convective heat transfer in rectangular enclosures driven by a continuously moving horizontal plate. International Journal of Heat and Mass Transfer, 52(21-22): 5055-5063. http://dx.doi.org/10.1016/j.ijheatmasstransfer.2009.05.011

[5] Oztop, H.F., Dagtekin, I. (2004). Mixed convection in two-sided lid-driven differentially heated square cavity. International Journal of Heat and Mass Transfer, 47(8-9): 1761-1769. http://dx.doi.org/10.1016/j.ijheatmasstransfer.2003.10.016

[6] Khanafer, K.M., Al-Amiri, A.M., Pop, I. (2007). Numerical simulation of unsteady mixed convection in a driven cavity, using an externally excited sliding lid. European Journal of Mechanics B/Fluids, 26: 669-687. http://dx.doi.org/10.1016/j.euromechflu.2006.06.0 06

[7] Tiwari, R.K., Das, M.K. (2007). Heat transfer augmentation in a two-sided lid-driven differentially heated square cavity utilizing nanofluids. International Journal of Heat and Mass Transfer, 50(9-10): 2002-2018. http://dx.doi.org/10.1016/j.ijheatmasstransfer.2006.09.034

[8] Sharif, M.A.R. (2007). Laminar mixed convection in shallow inclined driven cavities with hot moving lid on top and cooled from bottom. Applied Thermal Engineering, 27(5-6): 1036-1042. http://dx.doi.org/10.1016/j.applthermaleng.2006.07.035

[9] Abdelkhalek, M.M. (2008). Mixed convection in a square cavity by a perturbation technique. Computational Materials Science, 42(2): 212-219. http://dx.doi.org/10.1016/j.commatsci.2007.07.004

[10] Munshi, M.J.H., Alim, M.A., Ali, M., Alam, M.S. (2017). A numerical study of mixed convection in square lid-driven with internal elliptic body and constant flux heat source on the bottom wall. Journal of Scientific Research, 9(2): 145-158. http://dx.doi.org/ 10.3329/jsr.v9i2.29644

[11] Torrance, K., Davis, R., Eike, K., Gill, P., Gutman D., Hsui, A., Lyons, S., Zien, H. (1972). Cavity flows driven by buoyancy and shear. Journal of Fluid Mechanics, 51(2): 221-231. http://dx.doi.org/10.1017/s0022112072001181

[12] Iwatsu, R., Hyun, J.M., Kuwahara, K. (1993). Mixed convection in a driven cavity with a stable vertical temperature gradient. International Journal of Heat and Mass Transfer, 36(6): 1601-1608. http://dx.doi.org/10.1016/S0017-9310(05)80069-9

[13] Khanafer, K., Chamkha, A.J. (1999). Mixed convection flow in a lid-driven enclosure filled with a fluid-saturated porous medium. International Journal of Heat and Mass Transfer, 42(13): 2465-2481. http://dx.doi.org/10.1016/S0017-9310(98)00227-0

[14] Aydm, O. (1999). Aiding and opposing mechanisms of mixed convection in a shear- and buoyancy-driven cavity. International Communications in Heat and Mass Transfer, 26(7): 1019-1028. http://dx.doi.org/10.1016/S0735-1933(99)00091-3

[15] Ouertatani, N., Cheikh, N.B., Beya, B.B., Lili, T., Campo, A. (2009). Mixed convection in a double lid-driven cubic cavity. International Journal of Thermal Sciences, 48(7): 1265-1272. http://dx.doi.org/10.1016/j.ijthermalsci.2008.11.020

[16] Sivakumar, V., Sivasankaran, S., Prakash, P., Lee, J. (2010). Effect of heating location and size on mixed convection in lid-driven cavities. Computer and Mathematics with Applications, 59(9): 3053-3065. http://dx.doi.org/10.1016/j.camwa.2010.02.025

[17] Yapici, K., Obut, S. (2015). Laminar mixed-convection heat transfer in a lid-driven cavity with modified heated wall. Heat Transfer Engineering, 36(3): 303-314. http://dx.doi.org/10.1080/01457632.2014.916160

[18] Nosonov, I.I., Sheremet, M.A. (2018). Conjugate mixed convection in a rectangular cavity with a local heater. International Journal of Mechanical Sciences, 136: 243-251. http://dx.doi.org/10.1016/j.ijmecsci.2017.12.049

[19] Gangawane, K.M., Oztop, H.F. (2020). Mixed convection in the semi-circular lid-driven cavity with heated curved wall subjugated to constant heat flux for non-Newtonian power-law fluids. International Communications in Heat and Mass Transfer, 114: 104563. http://dx.doi.org/10.1016/j.icheatmasstransfer.2020.104563

[20] Park, H.M., Ryu, D.H. (2001). Rayleigh-Bénard convection of viscoelastic fluids in finited domains. Journal of Non-Newtonian Fluid Mechanics, 98: 169-184. http://dx.doi.org/10.1016/s0377-0257(01)00104-5

[21] Ohta, M., Ohta, M., Akiyoshi, M., Obata, E. (2002). A numerical study on natural convective heat transfer of

pseudoplastic fluids in a square cavity. Numerical Heat Transfer, Part A/Applications, 41(4): 357-372. http://dx.doi.org/10.1080/104077802317261218
[22] Inaba, H., Dai, C., Horibe, A. (2003). Natural convection heat transfer of microemulsion phase-change-material slurry in rectangular cavities heated from below and cooled from above. International Journal of Heat and Mass Transfer, 46(23): 4427-4438. http://dx.doi.org/10.1016/s0017-9310(03)00289-8
[23] Lamsaadi, M., Naïmi, M., Hasnaoui, M. (2005). Natural convection of non-Newtonian power law fluids in a shallow horizontal rectangular cavity uniformly heated from below. Heat and Mass Transfer, 41(3): 239-249. http://dx.doi.org/10.1007/s00231-004-0530-8
[24] Zhang, J., Vola, D., Frigaard, I.A. (2006). Yield stress effects on Rayleigh-Bénard convection. Journal of Fluid Mechanics, 566: 389-419. http://dx.doi.org/10.1017/S002211200600200X
[25] Balmforth, N.J., Rust, A.C. (2009). Weakly nonlinear viscoplastic convection. Journal of Non-Newtonian Fluid Mechanics, 158(1-3): 36-45. http://dx.doi.org/10.1016/j.jnnfm.2008.07.012
[26] Vikhansky, A. (2010). Thermal convection of a viscoplastic liquid with high Rayleigh and Bingham numbers. Physics of Fluids, 21(10): 103103. http://dx.doi.org/10.1063/1.3256166
[27] Akçay, M., Yükselen, M. (1999). Drag reduction of a nonnewtonian fluid by fluid injection on a moving wall. Archive of Applied Mechanics, 69(3): 215-225. http://dx.doi.org/10.1007/s004190050215
[28] Khani, F., Darvishi, M.T., Gorla, R.S.R. (2011). Analytical investigation for cooling turbine disks with a non-Newtonian viscoelastic fluid. Computers and Mathematics with Applications, 61(7): 1728-1738. http://dx.doi.org/10.1016/j.camwa.2011.01.040
[29] Krishnan, S., Aravamudan, K. (2013). Simulation of non-Newtonian fluid-food particle heat transfer in the holding tube used in aseptic processing operations. Food and Bioproducts Processing, 91(2): 129-148. http://dx.doi.org/10.1016/j.fbp.2012.08.008
[30] Foong, L.K., Shirani, N., Toghraie, D., Zarringhalam, M., Afrand, M. (2020). Numerical simulation of blood flow inside an artery under applying constant heat flux using Newtonian and non-Newtonian approaches for biomedical engineering. Computer Methods and Programs in Biomedicine, 190: 105375. http://dx.doi.org/10.1016/j.cmpb.2020.105375
[31] Niranjan, H., Sivasankaran, S., Bhuvaneswari, M. (2017). Chemical reaction, Soret and dufour effects on MHD mixed convection stagnation point flow with radiation and slip condition. Scientia Iranica B, 24(2): 698-706. http://dx.doi.org/10.24200/SCI.2017.4054
[32] Sivasankaran, S., Niranjan, H., Bhuvaneswari, M. (2017). Chemical reaction, radiation and slip effects on MHD mixed convection stagnation-point flow in a porous medium with convective boundary condition. International Journal of Numerical Methods for Heat and Fluid Flow, 27(2): 454-470. http://dx.doi.org/10.1108/HFF -02-2016-0044
[33] Badruddin, I.A., Zainal, A., Narayana, P.A.A., Seetharamu, K.N. (2006). Heat transfer in porous cavity under the influence of radiation and viscous dissipation. International Communications in Heat and Mass Transfer, 33(4): 491-499. http://dx.doi.org/10.1016/j.icheatmasstransfer.2006.01.015
[34] Prasad, V.R., Reddy, N.B., Muthucumaraswamy, R. (2007). Radiation and mass transfer effects on two-dimensional flow past an impulsively started infinite vertical plate. International Journal of Thermal Sciences, 46(12): 1251-1258. http://dx.doi.org/10.1016/jijthermalsci. 2007.01.004
[35] Mansour, M.A., Abd El-Aziz, M.M., Mohamed, R.A., Ahmed, S.E. (2011). Numerical simulation of natural convection in wavy porous cavities under the influence of thermal radiation using a thermal non-equilibrium model. Transport in Porous Media, 86(2): 585-600. http://dx.doi.org/10.1007/s11242-010-9641-5
[36] Sheremet, M.A. (2018). Natural convection combined with thermal radiation in a square cavity filled with a viscoelastic fluid. International Journal of Numerical Methods for Heat and Fluid Flow, 28: 624-640. http://dx.doi.org/10.1108/HFF-02-2017-0059
[37] Stengel, K.C., Oliver, D.S., Booker, J.R. (1982). Onset of convection in a variable-viscosity fluid. Journal of Fluid Mechanics, 120(1): 411-431. http://dx.doi.org/10.1017/S0022112082002821
[38] Richter, F.M., Nataf, H.C., Daly, S. (1983). Heat transfer and horizontally averaged temperature of convection with large viscosity variations. Journal of Fluid Mechanics, 129: 173-192. http://dx.doi.org/10.1017/S0022112083000713
[39] Busse, F.H., Frick, H. (1985). Square-pattern convection in fluids with strongly temperature-dependent viscosity. Journal of Fluid Mechanics, 150: 451-465. http://dx.doi.org/10.1017/S0022112085000222
[40] White, D.B. (1988). The plan forms and onset of convection with a temperature-dependent viscosity. Journal of Fluid Mechanics, 191: 247-286. http://dx.doi.org/10.1017/S0022112088001582
[41] Davaille, A., Jaupart, C. (1994). Onset of thermal convection in fluids with temperature-dependent viscosity: application to the oceanic mantle. Journal of Geophysical Research, 99(B10): 19853-19866. http://dx.doi.org/10.1029/94jb01405
[42] Zaranek, S.E., Parmentier, E.M. (2004). The onset of convection in fluids with strongly temperature-dependent viscosity cooled from above with implications for planetary lithospheres. Earth and Planetary Science Letters, 224(3-4): 371-386. http://dx.doi.org/10.1016/j.epsl.2004.05.013
[43] Kim, M.C., Choi, C.K. (2006). The onset of buoyancy driven convection in fluid layers with temperature-dependent viscosity. Physics of the Earth and Planetary Interiors, 155(1-2): 42-47. http://dx.doi.org/10.1016/j.pepi.2005.09.006
[44] Bottaro, A., Metzener, P., Matalon, M. (1992). Onset and two-dimensional patterns of convection with strongly temperature-dependent viscosity. Physics of Fluids A: Fluid Dynamics, 4(4): 655-663. http://dx.doi.org/10.1063/1.858283
[45] Astanina, M.S., Sheremet, M.A., Umavathi, J.C. (2015). Unsteady natural convection with temperature-dependent viscosity in a square cavity filled with a porous medium. Transport in Porous Media, 110(1): 113-126. http://dx.doi.org/10.1007/s11242-015-0558-x
[46] Alim, M.A., Alam, S., Miraj, M. (2014). Effects of volumetric heat source and temperature dependent

viscosity on natural convection flow along a wavy surface. Procedia Engineering, 90: 383-388. http://dx.doi.org/10.1016/j.proeng.2014.11.866

[47] Umavathi, J.C., Ojjela, O. (2015). Effect of variable viscosity on free convection in a vertical rectangular duct. International Journal of Heat and Mass Transfer, 84: 1-15. http://dx.doi.org/10.1016/j.ijheatmasstransfer.2014.12.066

[48] Amoura, M., Zeraibi, N., Smati, A., Gareche, M. (2006). Finite element study of mixed convection for non-Newtonian fluid between two coaxial rotating cylinders. International Journal of Heat and Mass Transfer, 33(6): 780-789. http://dx.doi.org/10.1016/j.icheatmasstransfer.2006.02.020

[49] Solomatov, V.S., Barr, A.C. (2007). Onset of convection in fluids with strongly temperature-dependent, power-law viscosity: 2. Dependence on the initial perturbation. Physics of the Earth and Planetary Interiors, 155(1-2): 1-13. http://dx.doi.org/10.1016/ j.pepi.2005.11.001

[50] Kaddiri, M., Naïmi, M., Raji, A., Hasnaoui, M. (2012). Rayleigh–Bénard convection of non-Newtonian power-law fluids with temperature-dependent viscosity. International Scholarly Research Network, ISRN Thermodynamics, 2012: 614712. http://dx.doi.org/10.5402/2012/614712

[51] Nouar, C. (2005). Thermal convection for a thermo-dependent yield stress fluid in an axisymmetric horizontal duct. International Journal of Heat and Mass Transfer, 48(25-26): 5520-5535. http://dx.doi.org/10.1016/j.ijheatmasstransfer.2005.06.016

[52] Scirocco, V., Devienne, R., Lebouché, M. (1985). Ecoulement laminaire et transfert de chaleur pour un fluide pseudo-plastique dans la zone d'entrée d'un tube. International Journal of Heat and Mass Transfer, 28: 91-99. http://dx.doi.org/10.1016/0017-9310(85)90011-0

[53] Balmforth, N.J., Craster, R.V. (2001). Geophysical aspects of non-Newtonian fluid mechanics. Geomorphological Fluid Mechanics, 34-51. http://dx.doi.org/10.1007/3-540-45670-8_2

[54] Siginer, D.A., Valenzuela-Rendon, A. (2000). On the laminar free convection and instability of grade fluids in enclosures. International Journal of Heat and Mass Transfer, 43(18): 3391-3405. http://dx.doi.org/10.1016/s0017-9310(99)00357-9

[55] Gray, D.D., Giorgini, A. (1976). The validity of the Boussinesq approximation for liquids and gases. International Journal of Heat and Mass Transfer, 19: 545-551. http://dx.doi.org/10.1016/0017-9310(76)90168-x

[56] Martyushev, S.G., Sheremet, M.A. (2012). Characteristics of Rosseland and P-1 approximations in modeling nonstationary conditions of convection-radiation heat transfer in an enclosure with a local energy source. Journal of Engineering Thermophysics, 21(2): 111-118. http://dx.doi.org/10.1134/s1810232812020026

[57] Magyari, E., Pantokratoras, A. (2011). Note on the effect of thermal radiation in the linearized Rosseland approximation on the heat transfer characteristics of various boundary layer flows. International Comm in Heat and Mass Transfer, 38(5): 554-556. http://dx.doi.org/10.1016/j.icheatmasstransfer.2011.03.006

[58] Ozoe, H., Churchill, S.W. (1972). Hydrodynamic stability and natural convection in Ostwald-De Waele and Ellis fluids: The development of a numerical solution. AIChE Journal, 18(6): 1196-1207. http://dx.doi.org/10.1002/aic.690180617

[59] Arroub, I., Bahlaoui, A., Raji, A., Hasnaoui, M., Naïmi, M. (2018). Cooling enhancement by nanofluid mixed convection inside a horizontal vented cavity submitted to sinusoidal heating. Engineering Computations, 35(4): 1747-1773. http://dx.doi.org/10.1108/EC-03-2017-0080

[60] Arroub, I., Bahlaoui, A., Raji, A., Hasnaoui, M., Naïmi, M. (2019). Varying heating effect on mixed convection of nanofluids in a vented horizontal cavity with injection or suction. Heat Transfer Engineering, 40(11): 941-958. http://dx.doi.org/10.1080/01457632.2018.1446876

[61] Arroub, I., Bahlaoui, A., Ezzaraa K., Raji, A., Hasnaoui, M., Naïmi, M. (2019). Effect of phase shift on mixed convection in a rectangular vented cavity filled with a nanofluid and submitted to periodic heating. Journal of Physics: Conference Series, 1226: 012001. http://dx.doi.org/10.1088/1742-6596/1226/1/012001

[62] Arroub, I., Bahlaoui, A., Belhouideg, S., Raji, A., Hasnaoui, M. (2021). Heat transfer performance in a tilted cavity submitted to external flow of nanofluid. AIP Publishing LLC, 2345: 020004. http://dx.doi.org/10.1063/5.0049447

[63] Roache, P.J. (1982). Computational Fluid Dynamics. Hermosa Publishers Albuquerque, New Mexico.

[64] Kefayati, G.R. (2015). FDLBM simulation of mixed convection in a lid-driven cavity filled with non-Newtonian nanofluid in the presence of magnetic field. International Journal of Thermal Sciences, 95: 29-46. http://dx.doi.org/10.1016/j.ijthermalsci.2015.03.018

[65] Karimipour, A., Nezhad, A. H., D'Orazio, A., Shirani, E. (2013). The effects of inclination angle and prandtl number on the mixed convection in the inclined lid driven cavity using Lattice Boltzmann method. Journal of Theoretical and Applied Mechanics, 51(2): 447-462.

[66] Moallemi, M.K., Jang, K.S. (1992). Prandtl number effects on laminar mixed convection heat transfer in a lid-driven cavity. International Journal of Heat and Mass Transfer, 35(8): 1881-1892. http://dx.doi.org/10.1016/0017-9310(92)90191-T

[67] Lamsaadi, M., Naïmi, M., Hasnaoui, M. (2006). Natural convection heat transfer in shallow horizontal rectangular enclosures uniformly heated from the side and filled with non-Newtonian power law fluids. Energy Conversion and Management, 47(15-16): 2535-2551. http://dx.doi.org/10.1016/j.enconman.2005.10.028

[68] Alloui, I., Benmoussa, H., Vasseur, P. (2010). Soret and thermosolutal effects on natural convection in a shallow cavity filled with a binary mixture. International Journal Heat and Fluid Flow, 31(2): 191-200. http://dx.doi.org/10.1016/j.ijheatfluidflow.2009.11.008

NOMENCLATURE

b	thermo-dependency coefficient
c_p	specific heat (J/kg.K)
g	gravitational acceleration (m/s^2)
Gr	Grashof number $\left(=\left(g\,\beta_T(T'_H - T'_C)L'^3\left[\left(\rho(u'_0 / L')^{n-1}\right)\right]\right)/k\right)$

k	consistency index for a power-law fluid at the reference temperature
L'	length of the cavity (m)
m	Pearson Number $\left(=-(1/K_T)/(dK_T/dT)\right)$
n	index of flow behavior for a power-law fluid
$\overline{Nu}$	average Nusselt number
Pr	Prandtl number $\left(=\left(c_p\, k\left(u_0'/L'\right)^{n-1}\right)/\lambda\right)$
q_r	radiation heat flux
R_d	the Radiation parameter $\left(=(4\sigma T_c^3)/(\lambda\beta_r)\right)$
Re	Reynolds number $\left(=\left(\rho\, L'^{n}\, u_0'^{2-n}\right)/k\right)$
Ri	Richardson number $\left(=Gr/Re^2=\left(g\beta(T_H'-T_C')L'\right)/\left(u_0'^2\right)\right)$
t	dimensionless time $\left(=t'u_0'/L'\right)$
T	dimensionless temperature $\left(=(T'-T_C')/(T_H'-T_C')\right)$
T'	dimensional temperature (K)
T_C'	temperature of the imposed inflow (K)
T_H'	dimensional hot temperature (K)
u_0'	the imposed flow's velocity (m/s)
(u, v)	dimensionless velocity components $\left(=(u',v')/u_0'\right)$
(x, y)	dimensionless coordinates $\left(=(x',\, y')/L'\right)$

Greek symbols

α	thermal diffusivity (m^2/s)
β_r	extinction coefficient, (m^{-1})
β_T	thermal expansion coefficient (1/K)
λ	thermal conductivity (W/(K.m))
μ	dynamic viscosity for a Newtonian fluid (Pa s)
μ_a	dimensionless apparent viscosity of fluid
ρ	Stephan-Boltzmann constant, ($Wm^{-2}K^{-4}$)
σ	dimensionless stream function $\left(=\Psi'/u_0'L'\right)$
Ψ	dimensionless vorticity $\left(=\Omega'\, L'/u_0'\right)$

Subscripts

C	cold temperature
H	hot temperature
max	maximum value
min	minimum value

Superscripts

$'$	dimensional variable